Biochemistry

pubs.acs.org/biochemistry Article

Biophysical Characterization of the Contribution of the Fab Region to the IgG-FcγRIIIa Interaction

Hirofumi Kosuge, Satoru Nagatoishi,* Masato Kiyoshi, Akiko Ishii-Watabe, Yosuke Terao, Teruhiko Ide, and Kouhei Tsumoto*

Cite This: *Biochemistry* 2023, 62, 262−269 Read Online

ACCESS | Metrics & More | Article Recommendations | Supporting Information

ABSTRACT: The cell-surface receptor FcγRIIIa is crucial to the efficacy of therapeutic antibodies as well as the immune response. The interaction of the Fc region of IgG molecules with FcγRIIIa has been characterized, but until recently, it was thought that the Fab regions were not involved in the interaction. To evaluate the influence of the Fab regions in a biophysical context, we carried out surface plasmon resonance analyses using recombinant FcγRIIIa ligands. A van't Hoff analysis revealed that compared to the interaction of the papain-digested Fc fragment with FcγRIIIa, the interaction of commercially available, full-length rituximab with FcγRIIIa had a more favorable binding enthalpy, a less favorable binding entropy, and a slower off rate. Similar results were obtained from analyses of IgG1 molecules and an IgG1-Fc fragment produced by Expi293 cells. For further validation, we also prepared a maltose-binding protein-linked IgG1-Fc fragment (MBP-Fc). The binding enthalpy of MBP-Fc was nearly equal to that of the IgG1-Fc fragment for the interaction with FcγRIIIa, indicating that such alternatives to the Fab domains as MBP do not positively contribute to the IgG-FcγRIIIa interactions. Our investigation strongly suggests that the Fab region directly interacts with FcγRIIIa, resulting in an increase in the binding enthalpy and a decrease in the dissociation rate, at the expense of favorable binding entropy.

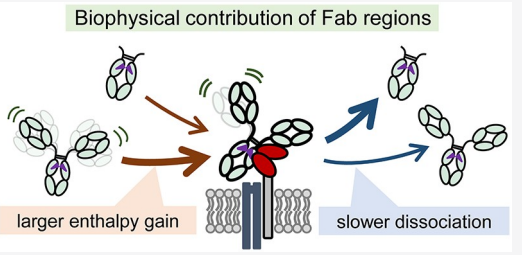

Antibodies are key players in the immune system. Due to the development of stable scaffolds that present regions with high specificity, antibody-based therapies are now clinically relevant.[1−3] The most abundant immunoglobulin in blood, IgG, consists of two Fab domains and an Fc domain linked through a flexible hinge region. The Fab portions are vital for the capture of a specific antigen, and the Fc region is necessary for the immune response triggered by the Fc-mediated interactions with complement factors and Fc receptors.[4−6] Although Fab and Fc domains work in concert, in many previous studies the biophysical functions of the domains have been examined independently. It is difficult to analyze the precise molecular function of intact IgG in part due to limited knowledge of the structure of full-length IgG.[7] To gain a better understanding of the molecular function of antibodies, the dynamics of full-length IgG occasionally with various ligands has recently been analyzed using various technologies, including computational methods.[7−11]

FcγRIIIa is an Fc receptor that mediates antibody-dependent cellular cytotoxicity (ADCC) through the interaction with IgG molecules.[4−6,12,13] The interaction between FcγRIIIa and the Fc region of IgG is well characterized as is the role of N-glycosylation of the Fc region.[5,12,14] The Fab regions were not thought to be relevant to the interaction until recently when Yogo et al. demonstrated the direct involvement of the Fab portion in the interaction between IgG and FcγRIIIa by using high-speed atomic force microscopy (HS-AFM) and hydrogen−deuterium exchange mass spectrometry (HDX-MS).[15] Sun et al. confirmed these findings by molecular dynamics (MD) simulation of the complex of full-length IgG1 with FcγRIIIa and by using hydroxyl radical footprinting mass spectrometry (HRF-MS).[11] The MD simulation demonstrated that one Fab portion directly interacts with FcγRIIIa regardless of core fucosylation.

To fully comprehend the mechanism of binding of the IgG ligand to FcγRIIIa, biophysical knowledge about the contribution of the Fab regions to the IgG-FcγRIIIa interaction is needed. To evaluate the impact of the Fab regions on the interaction of IgG with FcγRIIIa in the context of kinetic and thermodynamic parameters, we conducted the surface plasmon resonance (SPR) analyses using maltose-binding protein (MBP)[16,17] linked to an Fc fragment as well as full-length IgG1 and an Fc fragment. Our biophysical analyses strongly support the hypothesis that the Fab regions contribute to the interaction between IgG and FcγRIIIa and demonstrate that alternative components to the Fab domains, such as MBP, do

Special Issue: Protein Engineering

Received: December 31, 2021
Revised: April 20, 2022
Published: May 23, 2022

https://doi.org/10.1021/acs.biochem.1c00832
Biochemistry 2023, 62, 262−269

not stabilize the IgG-FcγRIIIa interaction. Our investigation thus provides information about the molecular mechanism of the IgG-FcγRIIIa interaction.

MATERIALS AND METHODS

Papain Digestion of Rituximab and Trastuzumab. Commercially available rituximab (Roche) was digested with papain in accordance with the manufacturer's protocol from the Pierce Fab Preparation Kit (Thermo Fisher Scientific). The papain-digested Fc fragment was purified by using an rProtein A Sepharose Fast Flow column (Cytiva) equilibrated with phosphate-buffered saline (PBS, pH 7.4). The column was washed with PBS, and the desired Fc fragment was eluted with Pierce IgG Elution Buffer (Thermo Fisher Scientific). The eluted fraction was neutralized by adding Tris-HCl (pH 8.0) to a final concentration of 100 mM, and the Fc fragment was further purified by size-exclusion chromatography using a HiLoad 16/600 Superdex 200 pg column (Cytiva) equilibrated with PBS (pH 7.4). Commercially available trastuzumab (Roche) was also digested with papain. The Fc fragment was purified using an rProtein A Sepharose Fast Flow column (Cytiva) with the same protocol that was used for rituximab. The Fc fragment was further purified by cation exchange chromatography using a Resource S column (Cytiva) to separate the Fc fragment from the Fab fragment. Mobile phase A consisted of 20 mM sodium acetate and 20 mM NaCl (pH 5.0), and mobile phase B consisted of 20 mM sodium acetate and 250 mM NaCl (pH 5.0). A linear gradient (from 0% to 100% B) was used (gradient length of 50 column volumes). The Fc fragment was finally purified by size-exclusion chromatography using a HiLoad 16/600 Superdex 200 pg column (Cytiva) equilibrated with PBS (pH 7.4).

Expression and Purification of Wild-Type FcγRIIIa. The DNA sequence encoding the human FcγRIIIa (V158) ectodomain (amino acid residues 1−175) with a C-terminal hexahistidine tag was cloned into the pcDNA3.4 vector (Thermo Fisher Scientific). Expi293 cells (Thermo Fisher Scientific) were transiently transfected with the vectors using the ExpiFectamine 293 Transfection Kit (Thermo Fisher Scientific) according to the manufacturer's protocol. The cells were cultured by rotating at 125 rpm for 5 days after transfection at 37 °C and 8% CO_2. The culture supernatant was collected by centrifugation at 1000*g* for 10 min and filtration. The collected supernatant was loaded onto a Ni-NTA agarose affinity column (Qiagen) after equilibration with binding buffer [20 mM Tris-HCl (pH 8.0), 500 mM NaCl, and 5 mM imidazole]. The resin capturing wild-type (WT) FcγRIIIa was washed with binding buffer, and subsequently, the protein was eluted with the buffers containing increasing concentrations of imidazole (≤500 mM). WT FcγRIIIa was obtained after further purification by size-exclusion chromatography using a HiLoad 16/600 Superdex 200 pg column (Cytiva) equilibrated with 50 mM Tris-HCl (pH 8.0), 500 mM NaCl, and 1 mM EDTA.

Expression and Purification of Mutant FcγRIIIa. The human FcγRIIIa (V158) ectodomain (amino acid residues 1−175) that has nine amino acid mutations with a C-terminal hexahistidine tag in the pTrc99a vector (Cytiva) was used to prepare mutant (Mut) FcγRIIIa as described previously.[18,19] The expression vector was transformed into *Escherichia coli* strain BL21 (DE3), and the cells were precultured in 3 mL of Luria-Broth medium overnight at 37 °C. The cells were further grown in 1 L of 2XYT medium at 37 °C until the OD_{600} reached ∼0.5. At that point, to induce protein expression, the cells were cultured with 0.2 mM isopropyl β-D-1-thiogalactopyranoside via rotation at 100 rpm overnight at 20 °C. The cultures were centrifuged at 8000*g* for 10 min at 4 °C. The harvested cell pellet was resuspended in binding buffer [20 mM Tris-HCl (pH 8.0), 500 mM NaCl, and 5 mM imidazole], and the cells were lysed with an ultrasonic cell-disrupting UD-201 instrument (TOMY). The cell lysate was centrifuged at 40000*g* for 30 min at 4 °C, and the soluble fraction was collected and filtered. The collected supernatant was loaded onto a Ni-NTA agarose affinity column (Qiagen) after equilibration with binding buffer [20 mM Tris-HCl (pH 8.0), 500 mM NaCl, and 5 mM imidazole]. The resin capturing Mut FcγRIIIa was washed with binding buffer, and subsequently, the protein was eluted with the buffers containing increasing concentrations of imidazole (≤500 mM). The eluted fractions containing Mut FcγRIIIa were further purified by size-exclusion chromatography using a HiLoad 16/600 Superdex 75 pg column (Cytiva) equilibrated with 50 mM Tris-HCl (pH 8.0), 500 mM NaCl, and 1 mM EDTA.

Expression and Purification of Expi293-Derived Antibodies. The DNA sequences of each antibody construct were cloned into the pcDNA3.4 vector (Thermo Fisher Scientific). Expi293 cells (Thermo Fisher Scientific) were transiently transfected with the vectors using ExpiFectamine 293 Transfection Kit (Thermo Fisher Scientific) according to the manufacturer's protocol. The cells were cultured by rotation at 125 rpm for 3−4 days after transfection at 37 °C and 8% CO_2. The culture supernatant was collected by centrifugation at 1000*g* for 10 min and filtration. The collected supernatant was loaded onto an rProtein A Sepharose Fast Flow resin (Cytiva) equilibrated with PBS (pH 7.4). The resin was washed with PBS (pH 7.4), and subsequently, the captured proteins were eluted with Pierce IgG Elution Buffer (Thermo Fisher Scientific). To neutralize the acidic eluates, Tris-HCl (pH 8.0) was added to the eluted fractions to a final concentration of 100 mM. The final purifications of the recombinant antibodies were performed by size-exclusion chromatography using a HiLoad 16/600 Superdex 200 pg column (Cytiva) in PBS (pH 7.4).

Surface Plasmon Resonance. The binding of each antibody to FcγRIIIa was analyzed using SPR on a Biacore T200 instrument (Cytiva). BSA-free Penta·His Antibody (Qiagen) was immobilized on a CM5 Biacore sensor chip (Cytiva) at 10000−13000 RU, after activation with *N*-hydroxysuccinimide/*N*-ethyl-*N*′-[3-(dimethylamino)propyl]-carbodiimide hydrochloride. After immobilization, the activated surface of the sensor chip was subsequently blocked by treatment with 1 M ethanolamine hydrochloride (pH 8.5). To measure the interaction of each antibody with FcγRIIIa, after 10 nM WT or Mut FcγRIIIa was captured on the sensor chip by the immobilized Penta·His Antibody at a flow rate of 10 μL/min for around 50 RU of capture level at the beginning of each cycle, a range of concentrations of each antibody (0.156−10 μM) were injected at a flow rate of 30 μL/min with a 90 s association time and a 180 s dissociation time. PBS (pH 7.4) containing 0.005% (v/v) Tween 20 was used as the running buffer. At the end of each cycle, the regeneration procedure was conducted by treatment with 1 M Arg-HCl (pH 4.4). The assay was performed at different temperatures. Using the BIAevaluation software (Cytiva), data analysis was carried out. A global fitting analysis assuming a 1:1 Langmuir binding

https://doi.org/10.1021/acs.biochem.1c00832
Biochemistry 2023, 62, 262−269

model determined association rate constants (k_{on}) and dissociation rate constants (k_{off}) for the interactions of WT and Mut FcγRIIIa. The dissociation constant (K_D) of the interaction was calculated by the following formula:

$$K_D = k_{off}/k_{on}$$

In addition, with regard to the interaction of WT FcγRIIIa, the dissociation constant was also calculated by fitting the equilibrium curve of steady-state affinity analysis for the van't Hoff plots. We statistically evaluated whether the differences in each parameter determined by the SPR analysis were significant as determined by a t test. The significant level was set to 0.05. The changes in enthalpy ($\Delta H°$) and entropy ($\Delta S°$) were calculated from the slope and intercept of the temperature dependence of the dissociation constant determined using the van't Hoff formula:

$$\ln K_D = \Delta H°/RT - \Delta S°/R$$

where R is the gas constant and T is the absolute temperature. On the basis of the calculated change in enthalpy and entropy, the change in Gibbs free energy ($\Delta G°$) was determined as follows:

$$\Delta G° = \Delta H° - T\Delta S°$$

Affinity Chromatography using a FcγRIIIa Column. Affinity chromatography was carried out using an affinity column [4.6 mm (inside diameter) × 75 mm] packed with a resin on which Mut FcγRIIIa was immobilized (TOSOH) as described previously[18,19] by an AKTA explorer instrument (Cytiva) with the measurement of absorbance at 280 nm. Mobile phase A consisted of 50 mM sodium citrate (pH 6.3), and mobile phase B consisted of 50 mM sodium citrate (pH 4.4). For analysis, 100 μg of each sample was applied to the FcγRIIIa affinity column after equilibration with mobile phase A. To elute the captured antibody ligands, the percentage of mobile phase B was increased by a linear gradient from 0% to 100% over 40 min at a flow rate of 0.5 mL/min, followed by 100% mobile phase B for 40 min.

Glycan Analysis. The composition of the N-glycan was determined using the analytical method with three steps: release of N-linked oligosaccharides, labeling with 2-aminobenzamide (2-AB), and UPLC. Using PNGase F (Roche), the N-linked oligosaccharides were separated from proteins. After the mixture of 20 μg of antibodies with 1 unit of PNGase F was incubated at 37 °C for 16 h, released N-linked oligosaccharides were applied to an Envi-Carb graphitized carbon column (Spelco) equilibrated with 1.0 mL of acetonitrile. The column was washed with 3.0 mL of water, and subsequently, the N-glycan was eluted with 1.0 mL of 5 mM ammonium acetate in 50% acetonitrile. The collected eluates were dried with a Savant SpeedVac centrifugal evaporator (Thermo Fisher Scientific). The dried samples were mixed with 10 μL of a labeling solution [0.37 M 2-AB and 1 M $NaCNBH_3$ in a 70:30 (v:v) DMSO/acetic acid mixture]. The reaction mixtures were incubated at 65 °C for 3 h, followed by gentle addition of 1.0 mL of acetonitrile. The sample was centrifuged at 15000g for 10 min, and the supernatant was discarded. The dissolved pellet in 20 μL of distilled water containing the labeled glycan was analyzed by UPLC using an ACQUITY UPLC BEH amide column (2.1 mm × 150 mm, 1.7 μm) by an ACQUITY UPLC H-class system (Waters). A total of 1 μL of sample was injected onto the column. To elute the labeled glycans, mobile phase A [0.1 M ammonium formate (pH 4.6)] and mobile phase B [100% (v/v) acetonitrile] were used with a linear gradient (25% A and 75% B to 50% A and 50% B) for 50 min. The fluorescence signals were detected at 420 nm (excited at 330 nm). On the basis of the previously reported elution profile,[20] the structure of the glycans corresponding to each peak was determined.

Circular Dichroism. To analyze the secondary structures of Expi293-derived IgG1-Fc and MBP-Fc, the circular dichroism (CD) spectra were recorded with a J-820 spectropolarimeter (Jasco) using the samples prepared at 0.1 mg/mL in PBS (pH 7.4) at 25 °C. The CD measurements were performed at a scanning speed of 20 nm/min by continuous scanning from 260 to 200 nm using a 1 mm path-length quartz cell. Five scans were recorded for each sample, and the collected data were analyzed by Spectra Analysis software (Jasco).

Differential Scanning Calorimetry. To analyze the thermal stabilities of Expi293-derived IgG1-Fc and MBP-Fc, differential scanning calorimetry (DSC) measurements were carried out using an automated PEAQ-DSC microcalorimeter (Malvern). Samples were prepared at 20 μM (IgG1-Fc) and 10 μM (MBP-Fc) in PBS (pH 7.4). The samples were loaded into the sample cell and heated from 10 to 100 °C at a rate of 60 °C/h. The collected data were analyzed with a non-two-state model by MicroCal PEAQ-DSC software (Malvern).

RESULTS AND DISCUSSION

Comparison of the Biophysical Parameters for Binding of Full-Length IgG1 and IgG1-Fc to FcγRIIIa. To interpret biophysically the influence of a Fab portion on IgG1-FcγRIIIa interaction, we carried out an SPR analysis using commercially available full-length rituximab (Roche). We also prepared the Fc fragment of rituximab by papain digestion to compare with full-length rituximab (Figure S1). We first used the recombinant WT FcγRIIIa ectodomain expressed by Expi293 cells as a ligand, and kinetic parameters of the interactions with full-length rituximab and rituximab-Fc were determined on the basis of curve fitting (Figure S2A and Table S1). Full-length rituximab had a higher affinity for WT FcγRIIIa than did rituximab-Fc, due to a slower dissociation rate. This result agrees with the results of previous HS-AFM analyses comparing the binding of FcγRIIIa to the full-length IgG and the Fc fragment.[15] Similarly, for the interaction with WT FcγRIIIa, commercially available full-length trastuzumab (Roche) also exhibited a dissociation rate that was slower than that of papain-digested trastuzumab-Fc (Figure S2B and Table S1).

Furthermore, on the basis of the measured binding affinities at different temperatures, thermodynamic parameters of the interactions of WT FcγRIIIa were calculated from van't Hoff plots. We could not obtain reliable thermodynamic parameters from the dissociation constants calculated by division of kinetic parameters, because the linear approximation could not be performed to van't Hoff plots. Therefore, on the basis of the dissociation constants calculated by the equilibrium curve fitting of steady-state affinity analysis at several temperatures (Figure S3A and Table S2), thermodynamic parameters of the interactions of WT FcγRIIIa with rituximab and rituximab-Fc were determined from van't Hoff plots (Figure S3B,C). The binding enthalpy of the interaction between WT FcγRIIIa and full-length rituximab was negatively larger, namely more favorable to stabilize the bound-state Gibbs free energy[21] than that with rituximab-Fc. In contrast, the binding entropy of

https://doi.org/10.1021/acs.biochem.1c00832
Biochemistry 2023, 62, 262−269

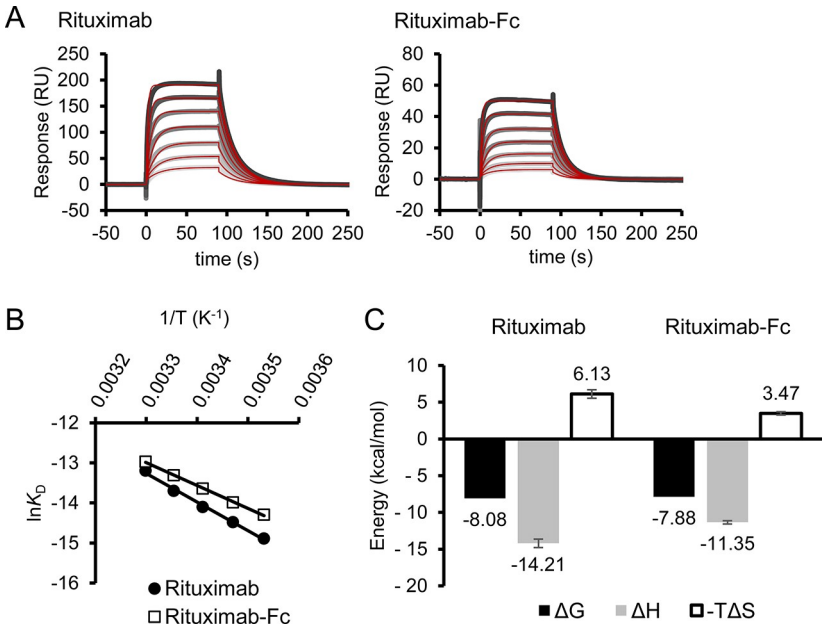

Figure 1. Analysis of the interactions of Mut FcγRIIIa with commercially available full-length rituximab and papain-digested rituximab-Fc. (A) SPR assay of the binding of rituximab and rituximab-Fc to Mut FcγRIIIa at 25 °C. The raw sensorgrams are shown as monochrome lines, and line darkness indicates concentration, with the darkest line showing the highest concentration. The curve fitting profiles are shown as red lines. (B) van't Hoff plots of the interactions of rituximab and rituximab-Fc with Mut FcγRIIIa. The average values of K_D at each temperature derived from at least three independent SPR measurements are plotted. The average values of K_D with standard errors are also listed in Table S3. R^2 values are more significant than 0.99 for both rituximab and rituximab-Fc. (C) Thermodynamic parameters of the interactions of rituximab and rituximab-Fc with Mut FcγRIIIa. Each parameter was determined from van't Hoff plots. Standard errors of linear fitting of van't Hoff plots are shown as error bars.

the interaction between full-length rituximab was negatively smaller, namely unfavorable compared with that with rituximab-Fc.

To further validate the role of the Fab domain, we carried out an SPR analysis using Mut FcγRIIIa. Mut FcγRIIIa contains nine mutations that increase stability in the absence of glycosylation and was produced by *E. coli* as described previously.[18,19] On the basis of curve fitting, kinetic parameters of the interactions were determined (Figure 1A and Table 1).

Table 1. Kinetic Parameters of the Interaction of Mut FcγRIIIa with Commercially Available Full-Length Rituximab and Papain-Digested Rituximab-Fc at 25 °C[a]

	k_{on} ($\times 10^4$ M^{-1} s^{-1})	k_{off} ($\times 10^{-2}$ s^{-1})	K_D ($\times 10^{-6}$ M)
rituximab	4.45 ± 0.12	4.98 ± 0.09	1.12 ± 0.03
rituximab-Fc	4.39 ± 0.23	7.21 ± 0.19	1.66 ± 0.08

[a]Four independent measurements were carried out. The average values with standard errors are given.

Full-length rituximab had a higher affinity for Mut FcγRIIIa than did rituximab-Fc, due to a slower dissociation rate, following the results of WT FcγRIIIa. On the basis of the measured binding affinities at different temperatures (Table S3), thermodynamic parameters of the interactions of Mut FcγRIIIa were also calculated from van't Hoff plots (Figure 1B,C). Following the results of WT FcγRIIIa, for the interaction with Mut FcγRIIIa, the binding enthalpy was more favorable and the binding entropy less favorable for full-length rituximab than for rituximab-Fc.

Interestingly, WT and Mut FcγRIIIa had quite different thermodynamic properties. When we compared the thermodynamic parameters of binding to antibody ligands, WT FcγRIIIa had more favorable binding entropy and a less favorable enthalpy than did Mut FcγRIIIa. The mutated residues of Mut FcγRIIIa are not located in the binding interface of FcγRIIIa with IgG-Fc. Comparison of previously reported crystal structures of glycosylated WT FcγRIIIa and nonglycosylated Mut FcγRIIIa did not show significant differences in the contact interface of the protein and N-glycan portions of IgG-Fc with FcγRIIIa.[18] This suggests that the different thermodynamic parameters between WT and Mut FcγRIIIa were due to the heterogeneous glycosylation of WT FcγRIIIa as shown from Figure S1. On the contrary, an enthalpy gain and an entropy loss of full-length rituximab compared with rituximab-Fc were observed for the interactions with both WT and Mut FcγRIIIa, indicating that the contribution of Fab regions does not depend on the glycosylation of FcγRIIIa. Therefore, using Mut FcγRIIIa should more clearly describe the influence of Fab regions by separating the protein interactions from the heterogeneous glycan interactions and be effective in evaluation of the contribution of Fab regions to IgG-FcγRIIIa interaction.

Interaction Analysis of the Antibody Ligands Expressed by Expi293 Cells. We further investigated the contribution of the Fab regions of IgG to the interaction with FcγRIIIa using three IgG1 antibodies (rituximab, trastuzumab, and adalimumab) and the IgG1-Fc fragment. The Fc regions of these ligands have the same amino acid sequence (Figure S4), and all were produced by Expi293 cells. No significant differences in separation profiles of these ligands isolated from Expi293 cells were observed by affinity chromatography using an FcγRIIIa affinity column packed with Mut FcγRIIIa-immobilized resin[18,19] (Figure S5), according to a glycan analysis that showed almost no differences in the Fc glycosylation patterns of these ligands (Figure S6).

https://doi.org/10.1021/acs.biochem.1c00832
Biochemistry 2023, 62, 262−269

We previously evaluated the interactions of Expi293-derived rituximab and trastuzumab with Mut FcγRIIIa using SPR analysis.[19] For this study, we conducted further SPR analyses to evaluate the interactions of the antibody ligands produced by Expi293 cells with Mut FcγRIIIa. In accordance with the kinetic difference between full-length rituximab and rituximab-Fc, all three full-length monoclonal antibodies dissociated more slowly from Mut FcγRIIIa than did IgG1-Fc, but binding affinities were not necessarily higher than that for IgG1-Fc (Table 2). The different binding affinities of the three full-length monoclonal antibodies might be caused by the different amino acid sequences in the joint region connecting the Fab portion to the upper hinge (Figure S4), as inferred from a previous study that reported the influence of the upper hinge region of human IgG1 on FcγRIIIa binding and ADCC activity.[22] As a side note, kinetic parameters of the interactions of WT FcγRIIIa with the antibody ligands produced by Expi293 cells determined by SPR analyses also indicated a tendency similar to that of Mut FcγRIIIa (Table S4).

Table 2. Kinetic Parameters of the Interaction between Mut FcγRIIIa and Expi293-Derived Antibody Ligands at 25 °C[a]

	k_{on} ($\times 10^4$ M^{-1} s^{-1})	k_{off} ($\times 10^{-2}$ s^{-1})	K_D ($\times 10^{-6}$ M)
rituximab[b]	3.96 ± 0.11	5.44 ± 0.11	1.38 ± 0.04
trastuzumab[b]	3.00 ± 0.10	5.83 ± 0.16	1.95 ± 0.05
adalimumab	4.00 ± 0.19	6.20 ± 0.37	1.55 ± 0.05
IgG1-Fc	4.78 ± 0.10	8.02 ± 0.17	1.68 ± 0.07
MBP-Fc	1.84 ± 0.05	6.35 ± 0.08	3.47 ± 0.10

[a]At least five independent measurements were carried out. The average values with standard errors are shown. [b]Data from our previous study.[19]

We next evaluated thermodynamic parameters of the interactions between Expi293-derived antibody ligands and Mut FcγRIIIa by van't Hoff analysis (Figure 2 and Table S5). In agreement with the differences between rituximab and rituximab-Fc, three full-length monoclonal antibodies had more favorable binding enthalpy and less favorable binding entropy than did the IgG1-Fc fragment, regardless of the difference in the Fab domain.

Validation of the Role of the Fab Region in FcγRIIIa Binding Using MBP-Fc. For further interaction analysis, we prepared an Fc fusion construct of MBP (MBP-Fc), in which MBP replaces the Fab domain (Figure 3A and Figure S4). MBP-Fc was produced by Expi293 cells. The secondary structure and thermal stability were evaluated using CD and DSC, respectively. Compared with the IgG1-Fc fragment produced by Expi293 cells, the MBP-Fc consisted of a higher proportion of α-helix (Figure 3B), as expected given the known structure of the MBP portion.[16,23] We observed a slight decrease in the thermal stability of the CH2 region of MBP-Fc compared to the IgG1-Fc fragment (Figure 3C). The glycosylation profile of MBP-Fc was verified by affinity chromatography using the FcγRIIIa affinity column and a glycan analysis (Figures S5 and S6). There were almost no significant differences in major glycoforms present on MBP-Fc compared to those on the other Expi293-derived antibodies.

Using the MBP-Fc ligand, we carried out an SPR analysis to evaluate the interaction with Mut FcγRIIIa. MBP-Fc had a lower affinity for Mut FcγRIIIa than the other Expi293-derived antibody ligands, mainly due to a slower association rate (Table 2). This might be caused by differences in the electrostatic attraction. Unlike the MBP portion, the Fab regions are positively charged, which may electrostatically contribute to the faster on rate. We further evaluated the contributions of Fab and MBP regions to the interaction by determining the thermodynamic parameters of the interaction between MBP-Fc and Mut FcγRIIIa (Figure 3D,E and Table S5). The binding enthalpy of MBP-Fc was less favorable than those of rituximab, trastuzumab, and adalimumab but almost commensurate with that of the IgG1-Fc fragment. This result demonstrated that the MBP portion does not compensate for the binding enthalpy gained by the presence of the Fab region. MBP-Fc had shown intermediate binding entropy between those of the three full-length antibodies and the IgG1-Fc fragment.

Biophysical Interpretation of the Contribution of the Fab Region to IgG-FcγRIIIa Interactions. Our results demonstrate that the Fab region of IgG positively contributes to the favorable binding enthalpy of its interaction with FcγRIIIa. Several recent studies using different biophysical methods indicated that the Fab regions influence the binding

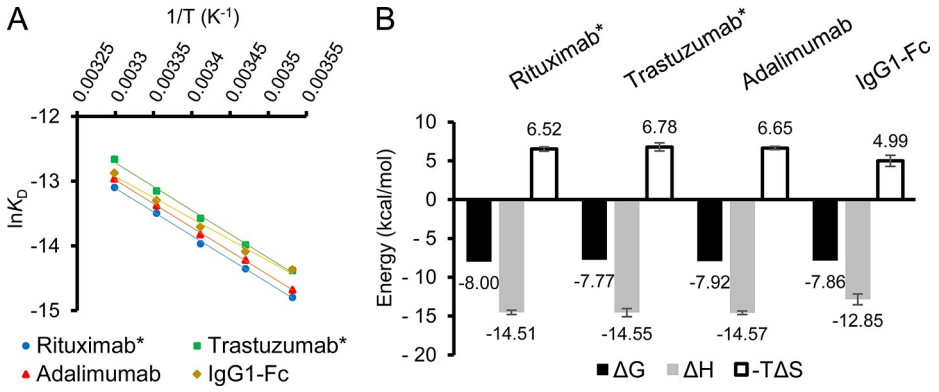

Figure 2. Thermodynamic parameters of the interactions between Mut FcγRIIIa and antibody ligands expressed in Expi293 cells measured by SPR. (A) van't Hoff plots of the interactions of Mut FcγRIIIa with rituximab (blue), trastuzumab (green), adalimumab (red), and IgG1-Fc (yellow). The average values of K_D at each temperature obtained from at least three independent SPR measurements are plotted. The average values of K_D with standard errors are also listed in Table S5. R^2 values are more significant than 0.99 for all of the ligands. (B) Thermodynamic parameters of the interactions between Mut FcγRIIIa and Expi293-derived antibody ligands. Each parameter was determined from van't Hoff plots. Standard errors of linear fitting of van't Hoff plots are shown as error bars. The asterisks indicate data reported in our previous study.[19]

https://doi.org/10.1021/acs.biochem.1c00832
Biochemistry 2023, 62, 262−269

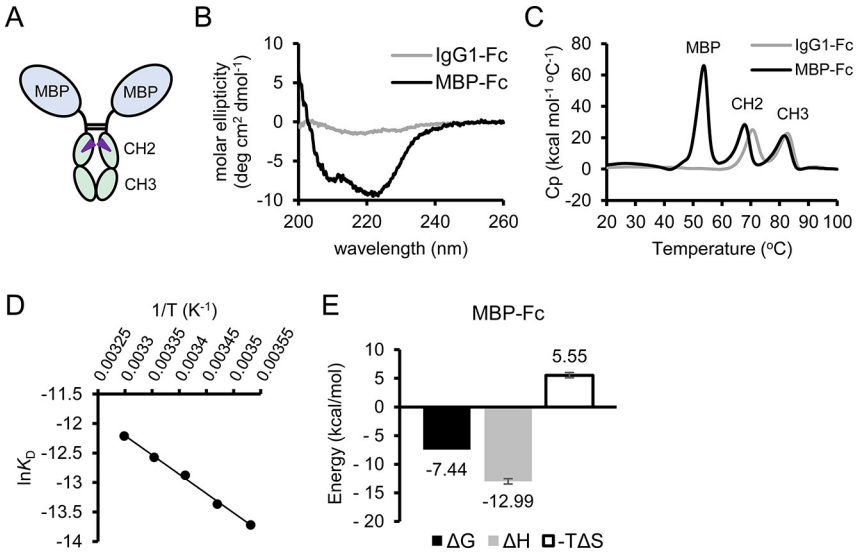

Figure 3. (A) Schematic of the MBP-Fc fusion. Purple triangles correspond to N-glycans. (B) CD spectra of MBP-Fc (black) and IgG1-Fc (gray). (C) DSC profiles of MBP-Fc (black) and IgG1-Fc (gray). (D) van't Hoff plots of the interaction between Mut FcγRIIIa and MBP-Fc. The average values of K_D at each temperature obtained from at least three independent SPR measurements at each temperature are plotted. The average values of K_D with standard errors are also listed in Table S5. R^2 values are >0.99. (E) Thermodynamic parameters of the interaction between Mut FcγRIIIa and MBP-Fc. Each parameter was determined from van't Hoff plots. Standard errors of linear fitting of van't Hoff plots are shown as error bars.

to FcγRIIIa.[11,15,24,25] The different solvent accessibilities between unbound and receptor-bound states of IgG have been previously assessed using HDX-MS,[15,24,25] HRF-MS,[11] and fast photochemical oxidation of proteins coupled with mass spectrometry.[24] The results of these analyses are contradictory in some cases, probably because of slight differences in the experimental conditions and analytical methods, but it seems clear that the solvent accessibility of the Fab region, especially the heavy chain, is decreased in the FcγRIIIa-bound state compared with the unbound state. The HS-AFM analysis by Yogo et al. revealed slower rates of dissociation of FcγRIIIa from intact IgG1 molecules than from the Fc fragment,[15] as we demonstrated using SPR kinetic analysis in this study. A breakthrough in understanding the contribution of the Fab region to the IgG-FcγRIIIa interaction was recently achieved by Sun et al. using MD simulation of the full-length IgG-FcγRIIIa complex.[11] In their simulations, they observed interactions of the FcγRIIIa D1 domain with the CH1 region of one Fab arm, in support of previous HDX-MS and HRF-MS analyses.[11,15,25] In combination with their MD-guided mutational study, this strongly suggests that Fab-FcγRIIIa interactions directly contribute to the modulation of ADCC activity.[11] Another MD simulation indicated that the CH1 domain of the Fab region of IgG1 interacts with the D1 domain of the high-affinity Fc receptor FcγRI.[9]

The results presented here provide strong support for direct interactions of the Fab region with FcγRIIIa from a thermodynamic perspective. We demonstrated that interactions of FcγRIIIa with full-length human IgG1 had more favorable binding enthalpy and less favorable binding entropy than did the interactions of FcγRIIIa with the IgG1-Fc fragment. Fab arms of IgG molecules can adopt a wide range of orientations due to the flexible hinge region. Given that a Fab segment is directly associated with FcγRIIIa, the dynamics of the Fab arm of receptor-bound IgG should be suppressed compared with that of unbound IgG, whereas binding enthalpy should be gained due to the additional Fab-FcγRIIIa interface (Figure 4). The enthalpy gain with Fab portions is also

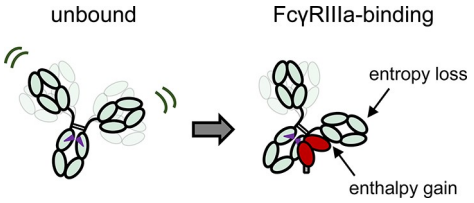

Figure 4. Model of the contributions of Fab portions to IgG-FcγRIIIa interaction. The red ovals correspond to ectodomains of FcγRIIIa. Purple triangles correspond to N-glycans.

strongly supported by our finding that the enthalpy change in binding of MBP-Fc to FcγRIIIa was no more favorable than that of the IgG1-Fc fragment to FcγRIIIa. In contrast, the binding entropy of the MBP-Fc-FcγRIIIa interaction was less favorable than that of the complex of the IgG1-Fc fragment with FcγRIIIa but more favorable than that of full-length IgG1-FcγRIIIa interactions. This was probably due to steric hindrance resulting from the MBP portion in the FcγRIIIa-bound state, although the MBP region did not interact with FcγRIIIa. Our result that the MBP portions did not contribute to the interaction with FcγRIIIa is an important finding for antibody engineering. This will provide an opportunity to reevaluate the utility of the IgG format with Fab domains for antibody drugs, while various antibodies different from IgG, including bispecific antibodies binding to both antigens and FcγRIIIa, are increasingly developed as antibody drugs at present.

Our biophysical analyses demonstrated that the Fab region enhances the binding enthalpy and reduces the dissociation rate of IgG-FcγRIIIa interaction, resulting in the stabilization of the interaction. In general, antibodies with slower dissociation rates for FcγRIIIa tend to show greater ADCC activities,[26,27] suggesting that the Fab region contributes to ADCC activities through the slow off rate of IgG-FcγRIIIa interactions. It is considered that the oligomerization and density of antigens affect the clustering of FcγRIIIa that is required for high ADCC activity.[28] When the antigens are monomers or the

https://doi.org/10.1021/acs.biochem.1c00832
Biochemistry 2023, 62, 262−269

antigen density is low on the cell surface, some IgG molecules should bind to the antigens using only one Fab portion. In that event, the other Fab portion is expected to touch FcγRIIIa and prevent rapid dissociation of the IgG molecule from FcγRIIIa, leading to increased ADCC activity.

Effector functions of IgG antibodies are elicited by the recruitment of leukocytes to antigen-presenting cells through the interactions with both the specific antigen and Fc receptors. There is debate regarding the intramolecular allostery between the variable region and constant region of IgG, which have an antigen binding function and effector function, respectively.[9,29−32] A previous study using MD simulations showed that antigen binding reduced the flexibility of the IgG1 antibody and resulted in a large reorientation of the Fab domains into two dominant conformational clusters with the open conformation of the CH2 domain ready for FcγRI binding; this suggested that antigen binding allosterically promotes the recognition of Fc receptors.[9] In accordance with this, more recent work demonstrated that antigen binding induces a conformational change in the Fc domain of IgG1, resulting in the enhancement of binding to FcγRIIIa.[29] Our work validated the biophysical interactions between IgG1 and FcγRIIIa in the absence of antigen binding. Given that the flexibility of antigen-bound antibodies is suppressed before FcγRIIIa binding, the interaction with FcγRIIIa antigen-bound IgG1 must have more favorable binding entropy than unbound IgG1. Thus, Fab portions of IgG1 are likely to contribute to IgG1-FcγRIIIa interaction in terms of not only Fab-FcγRIIIa contact but also antigen binding.

CONCLUSIONS

In summary, we assessed the contribution of the Fab region to the interactions between IgG1 and FcγRIIIa from kinetic and thermodynamic perspectives. The Fab region enhanced the binding enthalpy and reduced the dissociation rate, at the expense of favorable binding entropy. This biophysical interpretation indicates that there is direct contact between the Fab regions and FcγRIIIa and supports the hypothesis that antibody-mediated effector functions could be controlled through the modulation of the Fab region in addition to the Fc region. Our investigation enhances our understanding of the molecular functions of IgG antibodies with relevance to the engineering of therapeutic antibodies.

ASSOCIATED CONTENT

Supporting Information

The Supporting Information is available free of charge at https://pubs.acs.org/doi/10.1021/acs.biochem.1c00832.

Detailed information about the interaction analyses using SPR, sodium dodecyl sulfate−polyacrylamide gel electrophoresis of samples, amino acid sequences of antibody ligands we used, elution profile of FcγRIIIa affinity chromatography, and glycan analysis (PDF)

AUTHOR INFORMATION

Corresponding Authors

Satoru Nagatoishi − *The Institute of Medical Science, The University of Tokyo, Tokyo 108-8639, Japan; Center for Drug Design Research, National Institutes of Biomedical Innovation, Health and Nutrition, Ibaraki City, Osaka 567-0085, Japan;* orcid.org/0000-0002-0794-3963; Email: ngtoishi@ims.u-tokyo.ac.jp

Kouhei Tsumoto − *School of Engineering, The University of Tokyo, Tokyo 113-8656, Japan; The Institute of Medical Science, The University of Tokyo, Tokyo 108-8639, Japan; Center for Drug Design Research, National Institutes of Biomedical Innovation, Health and Nutrition, Ibaraki City, Osaka 567-0085, Japan;* orcid.org/0000-0001-7643-5164; Email: tsumoto@bioeng.t.u-tokyo.ac.jp

Authors

Hirofumi Kosuge − *School of Engineering, The University of Tokyo, Tokyo 113-8656, Japan*

Masato Kiyoshi − *Division of Biological Chemistry and Biologicals, National Institute of Health Sciences, Kawasaki, Kanagawa 210-9501, Japan*

Akiko Ishii-Watabe − *Division of Biological Chemistry and Biologicals, National Institute of Health Sciences, Kawasaki, Kanagawa 210-9501, Japan*

Yosuke Terao − *Tosoh Corporation, Ayase, Kanagawa 252-1123, Japan*

Teruhiko Ide − *Tosoh Corporation, Ayase, Kanagawa 252-1123, Japan*

Complete contact information is available at: https://pubs.acs.org/10.1021/acs.biochem.1c00832

Funding

This work was supported in part by JSPS KAKENHI-B Grant 20H02531 (to K.T.) and KAKENHIunder grant number 18H02082, 18H05425 (to S.N.) from the Japan Society for the Promotion of Science.

Notes

The authors declare no competing financial interest.

REFERENCES

(1) Goydel, R. S.; Rader, C. Antibody-based cancer therapy. *Oncogene* **2021**, *40*, 3655−3664.

(2) Goulet, D. R.; Atkins, W. M. Considerations for the Design of Antibody-Based Therapeutics. *J. Pharm. Sci.* **2020**, *109*, 74−103.

(3) Kaplon, H.; Reichert, J. M. Antibodies to watch in 2021. *mAbs* **2021**, *13*, 1860476.

(4) de Taeye, S. W.; Rispens, T.; Vidarsson, G. The Ligands for Human IgG and Their Effector Functions. *Antibodies* **2019**, *8*, 30.

(5) Caaveiro, J. M. M.; Kiyoshi, M.; Tsumoto, K. Structural analysis of Fc/FcγR complexes: A blueprint for antibody design. *Immunol. Rev.* **2015**, *268*, 201−221.

(6) Vidarsson, G.; Dekkers, G.; Rispens, T. IgG subclasses and allotypes : from structure to effector functions. *Front. Immunol.* **2014**, *5*, 520.

(7) Jay, J.; Bray, B.; Qi, Y.; Igbinigie, E.; Wu, H.; Li, J.; Ren, G. IgG Antibody 3D Structures and Dynamics. *Antibodies* **2018**, *7*, 18.

(8) Yanaka, S.; Yogo, R.; Kato, K. Biophysical characterization of dynamic structures of immunoglobulin G. *Biophys. Rev.* **2020**, *12*, 637−645.

(9) Zhao, J.; Nussinov, R.; Ma, B. Antigen binding allosterically promotes Fc receptor recognition. *MAbs* **2019**, *11*, 58−74.

(10) Zhang, X.; Zhang, L.; Tong, H.; Peng, B.; Rames, M. J.; Zhang, S.; Ren, G. 3D Structural Fluctuation of IgG1 Antibody Revealed by Individual Particle Electron Tomography. *Sci. Rep.* **2015**, *5*, 9803.

(11) Sun, Y.; Izadi, S.; Callahan, M.; Deperalta, G.; Wecksler, A. T. Antibody−receptor interactions mediate antibody-dependent cellular cytotoxicity. *J. Biol. Chem.* **2021**, *297*, 100826.

(12) Hanson, Q. M.; Barb, A. W. A perspective on the structure and receptor binding properties of immunoglobulin G Fc. *Biochemistry* **2015**, *54*, 2931−2942.

(13) Ganesan, L. P.; Cragg, M. S.; Vidarsson, G. Editorial : Roles of Fc Receptors in Disease and Therapy. *Front. Immunol.* **2020**, *11*, 1232.

(14) Shields, R. L.; Namenuk, A. K.; Hong, K.; Meng, Y. G.; Rae, J.; Briggs, J.; Xie, D.; Lai, J.; Stadlen, A.; Li, B.; Fox, J. A.; Presta, L. G. High Resolution Mapping of the Binding Site on Human IgG1 for FcγRI, FcγRII, FcγRIII, and FcRn and Design of IgG1 Variants with Improved Binding to the FcγR. *J. Biol. Chem.* **2001**, *276*, 6591−6604.
(15) Yogo, R.; Yamaguchi, Y.; Watanabe, H.; Yagi, H.; Satoh, T.; Nakanishi, M.; Onitsuka, M.; Omasa, T.; Shimada, M.; Maruno, T.; Torisu, T.; Watanabe, S.; Higo, D.; Uchihashi, T.; Yanaka, S.; Uchiyama, S.; Kato, K. The Fab portion of immunoglobulin G contributes to its binding to Fcγ receptor III. *Sci. Rep.* **2019**, *9*, 11957.
(16) Quiocho, F. A.; Spurlino, J. C.; Rodseth, L. E. Extensive features of tight oligosaccharide binding revealed in high-resolution structures of the maltodextrin transport/chemosensory receptor. *Structure* **1997**, *5*, 997−1015.
(17) Kapust, R. B.; Waugh, D. S. Escherichia coli maltose-binding protein is uncommonly effective at promoting the solubility of polypeptides to which it is fused. *Protein Sci.* **1999**, *8*, 1668−1674.
(18) Kiyoshi, M.; Caaveiro, J. M. M.; Tada, M.; Tamura, H.; Tanaka, T.; Terao, Y.; Morante, K.; Harazono, A.; Hashii, N.; Shibata, H.; Kuroda, D.; Nagatoishi, S.; Oe, S.; Ide, T.; Tsumoto, K.; Ishii-Watabe, A. Assessing the Heterogeneity of the Fc-Glycan of a Therapeutic Antibody Using an engineered FcγReceptor IIIa-Immobilized Column. *Sci. Rep.* **2018**, *8*, 3955.
(19) Kosuge, H.; Nagatoishi, S.; Kiyoshi, M.; Ishii-Watabe, A.; Tanaka, T.; Terao, Y.; Oe, S.; Ide, T.; Tsumoto, K. Highly sensitive HPLC analysis and biophysical characterization of N-glycans of IgG-Fc domain in comparison between CHO and 293 cells using FcγRIIIa ligand. *Biotechnol. Prog.* **2020**, *36*, e3016.
(20) Reusch, D.; Haberger, M.; Falck, D.; Peter, B.; Maier, B.; Gassner, J.; Hook, M.; Wagner, K.; Bonnington, L.; Bulau, P.; Wuhrer, M. Comparison of methods for the analysis of therapeutic immunoglobulin G Fc-glycosylation profiles — Part 2 : Mass spectrometric methods Comparison of methods for the analysis of therapeutic immunoglobulin G Fc-glycosylation profiles — Part 2 : Mass spect. *mAbs* **2015**, *7*, 732−742.
(21) Akiba, H.; Tsumoto, K. Thermodynamics of antibody-antigen interaction revealed by mutation analysis of antibody variable regions. *J. Biochem.* **2015**, *158*, 1−13.
(22) Yan, B.; Boyd, D.; Kaschak, T.; Tsukuda, J.; Shen, A.; Lin, Y.; Chung, S.; Gupta, P.; Kamath, A.; Wong, A.; Vernes, J. M.; Meng, G. Y.; Totpal, K.; Schaefer, G.; Jiang, G.; Nogal, B.; Emery, C.; Vanderlaan, M.; Carter, P.; Harris, R.; Amanullah, A. Engineering upper hinge improves stability and effector function of a human IgG1. *J. Biol. Chem.* **2012**, *287*, 5891−5897.
(23) Greenfield, N. J. Using circular dichroism collected as a function of temperature to determine the thermodynamics of protein unfolding and binding interactions. *Nat. Protoc.* **2006**, *1*, 2527−2535.
(24) Shi, L.; Liu, T.; Gross, M. L.; Huang, Y. Recognition of Human IgG1 by Fcγ Receptors: Structural Insights from Hydrogen-Deuterium Exchange and Fast Photochemical Oxidation of Proteins Coupled with Mass Spectrometry. *Biochemistry* **2019**, *58*, 1074−1080.
(25) Houde, D.; Peng, Y.; Berkowitz, S. A.; Engen, J. R. Post-translational modifications differentially affect IgG1 conformation and receptor binding. *Mol. Cell. Proteomics* **2010**, *9*, 1716−1728.
(26) Stavenhagen, J. B.; Gorlatov, S.; Tuaillon, N.; Rankin, C. T.; Li, H.; Burke, S.; Huang, L.; Johnson, S.; Bonvini, E.; Koenig, S. Fc Optimization of Therapeutic Antibodies Enhances Their Ability to Kill Tumor Cells In vitro and Controls Tumor Expansion In vivo via Low-Affinity Activating Fc ; Receptors. *Cancer Res.* **2007**, *67*, 8882−8890.
(27) Liu, Z.; Gunasekaran, K.; Wang, W.; Razinkov, V.; Sekirov, L.; Leng, E.; Sweet, H.; Foltz, I.; Howard, M.; Rousseau, A.; Kozlosky, C.; Fanslow, W.; Yan, W. Asymmetrical Fc Engineering Greatly Enhances Antibody- dependent Cellular Cytotoxicity (ADCC) Effector Function and Stability of the Modified Antibodies. *J. Biol. Chem.* **2014**, *289*, 3571−3590.
(28) Murin, C. D. Considerations of Antibody Geometric Constraints on NK Cell Antibody Dependent Cellular Cytotoxicity. *Front. Immunol.* **2020**, *11*, 1635.
(29) Orlandi, C.; Deredge, D.; Ray, K.; Gohain, N.; Tolbert, W.; DeVico, A. L.; Wintrode, P.; Pazgier, M.; Lewis, G. K. Antigen-Induced Allosteric Changes in a Human IgG1 Fc Increase Low-Affinity Fcγ Receptor Binding. *Structure* **2020**, *28*, 516−527.e5.
(30) Yang, D.; Kroe-Barrett, R.; Singh, S.; Roberts, C. J.; Laue, T. M. IgG cooperativity − Is there allostery ? Implications for antibody functions and therapeutic antibody development. *mAbs* **2017**, *9*, 1231−1252.
(31) Bowen, A.; Casadevall, A. Revisiting the Immunoglobulin Intramolecular Signaling Hypothesis. *Trends Immunol.* **2016**, *37*, 721−723.
(32) Janda, A.; Bowen, A.; Greenspan, N. S.; Casadevall, A. Ig Constant Region Effects on Variable Region Structure and Function. *Front. Microbiol.* **2016**, *7*, 22.

https://doi.org/10.1021/acs.biochem.1c00832
Biochemistry 2023, 62, 262−269